A&A 553, L10 (2013)
DOI: 10.1051/0004-6361/201321465

Astronomy & Astrophysics

Letter to the Editor

Hi-C and AIA observations of transverse magnetohydrodynamic waves in active regions⋆

R. J. Morton and J. A. McLaughlin

Department of Mathematics & Information Sciences, Northumbria University, Newcastle Upon Tyne, NE1 8ST, UK
e-mail: richard.morton@northumbria.ac.uk

Received 13 March 2013 / Accepted 30 April 2013

ABSTRACT

The recent launch of the High resolution Coronal imager (Hi-C) provided a unique opportunity of studying the EUV corona with unprecedented spatial resolution. We utilize these observations to investigate the properties of low-frequency (50−200 s) active region transverse waves, whose omnipresence had been suggested previously. The five-fold improvement in spatial resolution over SDO/AIA reveals coronal loops with widths 150−310 km and that these loops support transverse waves with displacement amplitudes <50 km. However, the results suggest that wave activity in the coronal loops is of low energy, with typical velocity amplitudes <3 km s^{-1}. An extended time-series of SDO data suggests that low-energy wave behaviour is typical of the coronal structures both before and after the Hi-C observations.

Key words. Sun: corona – Sun: chromosphere – waves – magnetohydrodynamics (MHD)

1. Introduction

There have now been numerous reports of ubiquitous magnetohydrodynamic (MHD) waves in the solar atmosphere. In particular the periodic, transverse displacement of magnetic flux tubes in both the chromosphere (De Pontieu et al. 2007; Kuridze et al. 2012; Morton et al. 2012) and in the corona (Tomczyk et al. 2007; Erdélyi & Taroyan 2008). The chromospheric motions are somewhat better resolved as they are observed with high-resolution (<0.″07 per pixel) imagers, e.g., space- (Hinode) and ground-based (ROSA, CRISP). The observations of coronal transverse waves, however, are typically restricted because of larger spatial resolutions, >0.″5 per pixel, and also because the coronal plasma is optically thin. Both these effects contribute to problems with line-of-sight (LOS) integration, meaning that several coronal structures may contribute to emission within a single pixel. This restriction has led to some differing results on the observed properties of the transverse waves. For example, velocity amplitudes of these waves are reported as ∼0.4 km s^{-1} in off-limb, active region loops (Coronal Multi-Channel Polarimeter/CoMP – Tomczyk et al. 2007), while observations with the Solar Dynamic Observatory (SDO) suggest typical amplitudes of ∼5 km s^{-1} (McIntosh et al. 2011). De Moortel & Pascoe (2012) demonstrated that LOS integration of multiple unresolved structures would lead to an underestimate of velocity amplitudes. However, their results suggest this does not account for the observed differences. Another solution is that current resolutions and cadences are masking the true nature of transverse waves. The data taken with the High resolution Coronal Imager (Cirtain et al. 2013) provide a unique opportunity of studying active region transverse waves at high resolution.

2. Observations and data reduction

The Hi-C observations took place on 12 July 2012 from 18:51:52 UT to 18:55:13 UT centred on an active region at (−130.″0, −453.″3) from disk centre. The images were obtained in the 193 Å passband (spectral width −5 Å). The data were taken with a cadence of ∼5.4 s and a spatial resolution of 0.″103 per pixel (∼75 km). Further details on the telescope can be found in Cirtain et al. (2013). We obtained the level 1.5, 4k × 4k data set through the Virtual Solar Observatory. The data were dark-subtracted, flat-fielded, cropped, dust-hidden and co-aligned by the Hi-C Science team. We found that the data still displayed visible shifts, so we additionally aligned the data using cross-correlation to achieve sub-pixel alignment. Testing the accuracy of the alignment suggests the remaining errors have a frame-to-frame RMS value of 0.05 pixels. The data are missing a frame between 18:54:12-18:54:23 UT, therefore we used linear interpolation to create the missing frame and provide a constant sampling rate for wave studies. Note that the first seven frames of the Hi-C data are inadequate for data analysis. They are displayed in figures and movies, but are not used for analysis.

The 193 Å line has strong contributions from Fe XII, which has a peak formation temperature close to 1.5 MK, which is ideal for observing coronal features. However, the images not only show well-defined coronal loops (Fig. 1), but also spicular and fibrillar structures in and around the moss regions. The data show that the spicules/fibrils are constantly in motion, displaying evidence of flows and waves. However, this is in contrast to a corona that shows relatively muted dynamic behaviour. To analyse the motions of the fine-structure we have manipulated the images slightly. Due to the low signal-to-noise ratio (S/N) of Hi-C, we first applied a spatial filtering algorithm to each frame to suppress the highest frequency spatial components to increase the S/N. We then applied a 5-by-5 box-car smoothing function to further suppress noise, while retaining sufficient signal to resolve the fine-scale structure. To highlight the fine-structure we used an unsharp mask procedure (see, e.g., Fig. 2).

Because of the short duration of the Hi-C time-series, we used additional data from the SDO Atmospheric Imaging Assembly (AIA; Lemen et al. 2011) to study the long-term behaviour of the region. The data represent a larger region around the Hi-C field of view, comprise of the 171 Å and 193 Å

⋆ Appendix A and five movies associated to Figs. A.2−A.6 are available in electronic form at http://www.aanda.org

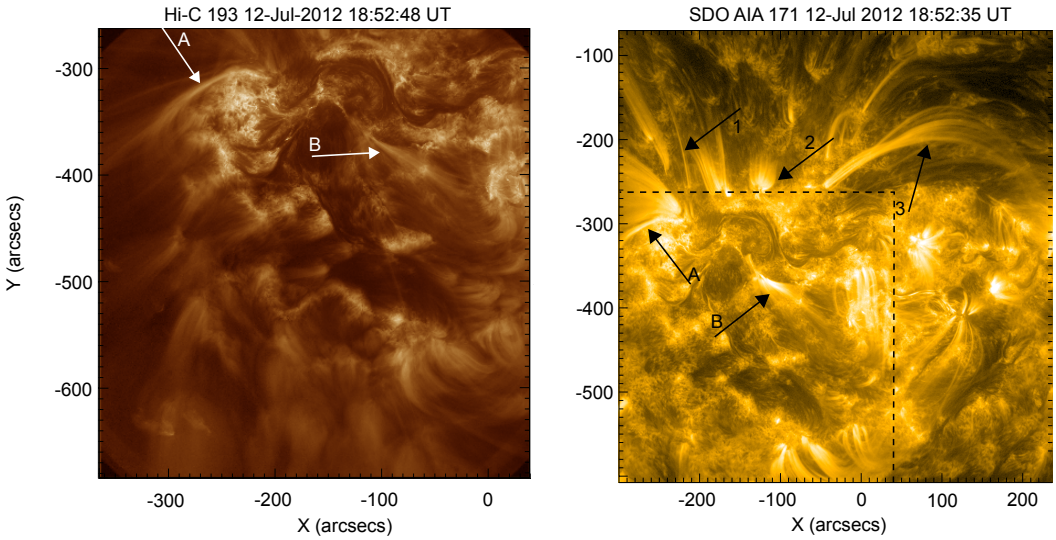

Fig. 1. Active region observed with Hi-C 193 Å (*left*) and SDO/AIA 171 Å (*right*). The displayed AIA field of view demonstrates the extended structure of the active region, and the dashed black box highlights the overlap with Hi-C. The arrows on the Hi-C image highlight the two coronal structures (labelled A and B) studied in high resolution in this paper. The same arrows are also shown on the AIA image, with the additional arrows labelled 1−3 highlighting the loop structures studied in AIA data only.

bandpasses, and cover the period 18:40:47−19:04:47 UT. The AIA data were prepared using the standard techniques; alignment and unsharp masking were also performed on the data sets.

3. Data analysis

We searched the data for signatures of transverse wave motion, i.e., the physical displacement of the structure's central axis. This was performed by placing a cross-cut perpendicular to the structure under consideration and producing a time-distance diagram. To analyse the structures in the time-distance diagrams, we fitted a Gaussian function to the cross-sectional flux profile in each time slice (see, e.g., Aschwanden & Schrijver 2011), which allows for sub-pixel accuracy on locating the central position of the structure's cross-section. The fitting of the Gaussian requires an estimate of the data noise (σ_N), which we calculated following Yuan & Nakariakov (2012),

$$\sigma_N = \sqrt{\sigma_p(F)^2 + \sigma_d^2 + \sigma_r^2 + \sigma_{sd}^2} = \sqrt{0.23F + 588.4}, \quad (1)$$

where $\sigma_p(F)$ is the uncertainty in photon noise, σ_d is the dark current, σ_r the readout and σ_{sd} the digitisation (priv. comm. – A. Winebarger). Similar formulae were used for the AIA data noise (Yuan & Nakariakov 2012). We also took into account errors in alignment between the frames. To determine the total error on position we added the alignment error to the Gaussian centroid position error, assuming the alignment error for each data point to be the RMS value of 0.05 pixels for Hi-C and 0.01 for AIA data. We then supplied a non-linear fitting algorithm with the central positions and the standard errors and instructed it to fit a function of the form

$$F(t) = A \sin\left(\frac{2\pi}{P}t - \phi\right) + g(t),$$

where A, P, and ϕ are the displacement amplitude, period, and phase, respectively, of the wave. The parameter $g(t)$ is a linear function that represents any transverse drift of the structure with time, which could possibly be attributed to long-period transverse waves. From the fitted parameters we calculated the velocity amplitude using the relation $v = 2\pi A/P$.

Numerous coronal structures can be observed in the Hi-C images. Two large, distinct coronal structures, arbitrarily labelled A and B, are easily identified at (−250″, −330″) and (−80″, −370″), respectively (Fig. 1 – highlighted by arrows). The rest of the coronal structures are fine loops with diffuse emission. The low S/N of the Hi-C data means that any fine-structure of these diffuse loops cannot be resolved. Hence, we concentrated on the distinct coronal structures.

Example time-distance diagrams for A and B are plotted in Fig. 2. Perhaps surprisingly, these structures show little visible evidence of periodic transverse motion. For the structure A, we show a time-distance diagram taken close to the loop apex (Fig. 2 – top panels). The filtering technique has revealed that this coronal structure consists of 6−7 fine threads. Fitting a Gaussian to the loop cross-sections gives loop widths of 150−310 km, suggesting that the fine structure is not clearly resolved in the corresponding AIA 193 Å images. This is confirmed because the unsharp masking of the AIA images does not reveal these individual loop threads (see online movies 1−4).

Upon applying the Gaussian fitting technique to the loops, we were able to resolve small amplitude transverse displacement towards the foot points of the loops in structure A. A sinusiodal fit suggests that the displacement is periodic (see, e.g., Fig. 3), where the measured displacement amplitude (47 ± 14 km) is a factor of 10 smaller than the AIA pixel size. The transverse displacements can be measured along a portion of the loop leg (∼2200 km) but overlapping loops prevented us from following the signal to the apex. The amplitude of the wave is seen to increase with height along the leg, from 25 km to 50 km. Cross-correlation of the signals in neighbouring slits suggests that the feature is propagating with phase speeds 400 ± 300 km s^{-1}. Transverse motion in a neighbouring loop in the legs also has a small displacement amplitude of A = 22 ± 12 km, with P = 65 ± 10 s. In contrast, measurements suggest the amplitude decreases with height. The identification of periodic transverse displacement towards the loop apex is more uncertain because of lower S/N. While the results of the fitting suggest transverse displacements with amplitudes of 10−25 km, there are large uncertainties in the fit parameters. The best example of the fits towards the loop apex is given in Fig. 2.

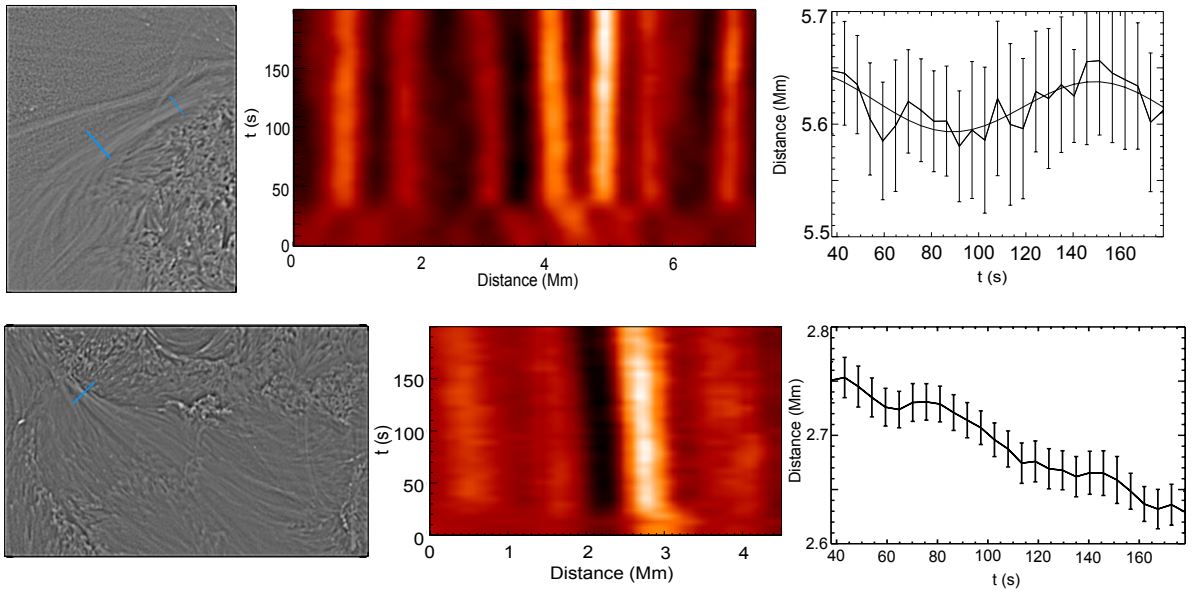

Fig. 2. *Top row*: *the left panel* displays close-up, filtered images of the coronal structures labelled A and *the middle panel* displays a time-distance diagram for a cross-cut at the loop apex, with the cross-cut position shown in *the left panel*. *The right panel* is the results of the fitting of a loop at the apex and has measured parameters of $P = 126 \pm 80$ s, $A = 25 \pm 22$ km and $v = 1.2 \pm 1.3$ km s^{-1}. *Bottom row*: *the left panel* displays close-up, filtered images of the coronal structures labelled B and *the middle panel* displays a time-distance diagram taken close to the footpoint, with the cross-cut position shown in *the left panel*. *The right panel* is the results of the fitting to the loop. The time-scales are given in seconds from the start of Hi-C observations.

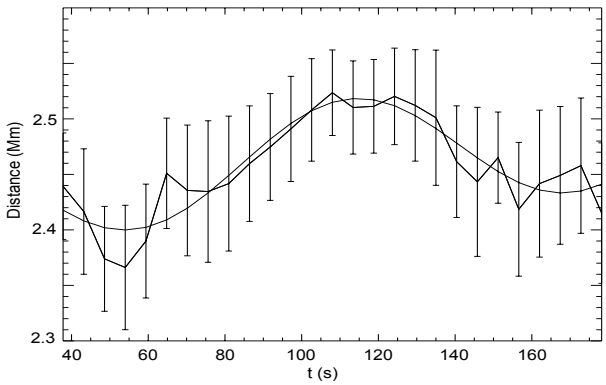

Fig. 3. Results from the fitting at the footpoint of structure A (position of cross-cut given in top left panel – Fig. 2). A sinusoidal fit to the data points has measured parameters of $P = 109 \pm 16$ s, $A = 50 \pm 14$ km and $v = 2.9 \pm 0.9$ km s^{-1}.

The changes in amplitude along the loop legs are interesting. Cross-correlation suggests the waves are propagating, implying an that initial increase in amplitude could be due to decreasing density with height. We speculate that the reduction in amplitude with height could be explained by spatial damping, e.g., by invoking resonant absorption as a damping mechanism for the transverse waves (Terradas et al. 2010; Pascoe et al. 2012). Verth et al. (2010) showed that resonant absorption is compatible with the decrease in propagating wave amplitude along coronal loops observed in CoMP (Tomczyk & McIntosh 2009). For propagating waves, competition between amplification and damping is expected to occur in the majority of loops, with the observable variation in amplitude dependent upon the individual loop.

In the second coronal structure labelled B (Fig. 2 – bottom row) there is no measurable periodic motion. The results from the fitting hint at very small amplitude periodic motion (Fig. 2: from 40–90 s), however, the total displacement is below the magnitude of the uncertainties, and therefore cannot be claimed as wave motion. The linear term in the sinusoidal fit, $g(t)$, may represent a transverse motion of the loop with a long period (>230 s). The apparent velocity amplitude of this transverse motion is ~1 km s^{-1}, however, we do not claim it is periodic wave motion. In Fig. 4, the time-distance diagram is shown for the AIA 193 Å data of the same spatial location. It demonstrates the activity for an extended period of time both before and after the Hi-C observations. Measurements suggest that the structure does not exhibit large amplitude wave activity during the AIA observations. However, we note that the coronal loop resolved in Hi-C has a width of ~230 km. This is smaller than an AIA pixel and thus AIA does not resolve the structure adequately in Fig. 4, which shows enhanced emission with a width of ~600 km, possibly indicating contributions from neighbouring features.

To gain a sense of typical wave activity in the active region, additional coronal structures in the AIA 171 Å images were studied (labelled 1–3 in Fig. 1). The features are partially visible in the Hi-C data only for a few frames because of the shift in pointing of the telescope. Figure 4 displays the time-distance diagrams produced for these features. The cross-cuts from structures 1 and 2 do not show any visible signs of transverse displacement. Applying the fitting routine suggests the presence of long-period ($P > 300$ s) and small-amplitude ($A < 100$ km, $v < 3$ km s^{-1}) waves. However, the feature labelled 3 is different and displays transverse motion that is visible even to the eye (online movie 5). A cross-cut is placed near the apex of this feature (close to arrow in Fig. 1) and reveals periodic motion in numerous loop threads. One example is highlighted (over-plotted black line) and the measured values are $P = 324 \pm 2$ s, $A = 331 \pm 4$ km, $v = 6.42 \pm 0.09$ km s^{-1}. However, the transverse wave motion does not appear to be continuous, and only one or two wave periods are visible before the perturbation decays. Note that this decay may not be due to damping, but rather that the observed motion is a wave-packet of finite length travelling through the cross-cut.

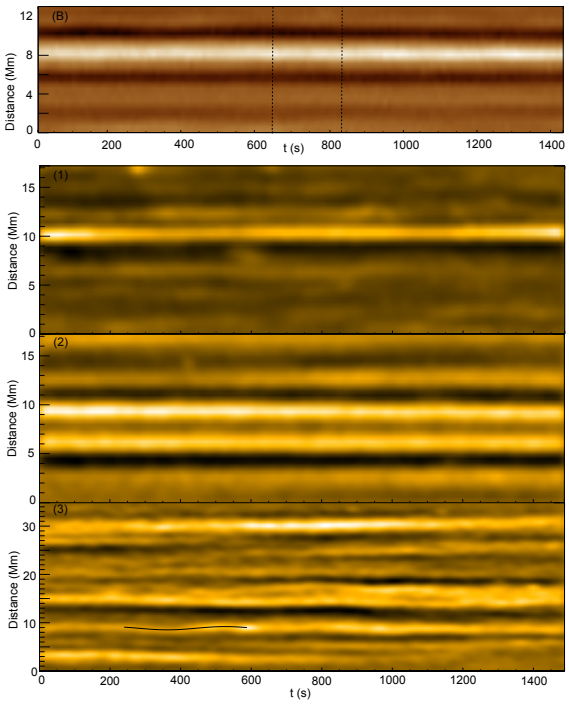

Fig. 4. Time-distance diagram of the coronal feature labelled B as seen with AIA 193 Å (*top panel*). The time of the Hi-C observations are marked by the dashed lines. The *second set of panels* displays time-distance diagrams for the coronal features identified as 1−3 in Fig. 1 as seen with AIA 171 Å. The time-scales are given in seconds from the start of the AIA observations.

4. Discussion and conclusions

With the five-fold increase in resolution of Hi-C we have been able to observe transverse periodic motion ($A < 50$ km) in coronal loops that would otherwise have been difficult with AIA. The Hi-C coronal loops have widths of the order of or below the AIA resolution and are not resolved by AIA. The Hi-C data only reveals small-amplitude, low-energy waves and some coronal structures do not show measurable periodic transverse motion even at high resolution.

The lack of identifiable wave motion in some Hi-C coronal loops could be limited by resolution still or data noise. Assuming the corona is filled with transverse waves and wave energy, our results allow us to place an upper bound on the amplitude of the transverse waves in some coronal active region structures. We suggest that transverse waves with an amplitude of $<0\farcs03$ (20 km) (i.e., total displacement is less than half a pixel ∼40 km) are at the edge of Hi-C observational limitations. Hence, any low-frequency waves present with periods in the range 50−200 s will have velocity amplitudes of <3 km s^{-1}.

A further reason for the absence of periodic transverse waves in some loops is due to the short length of the data set, ≈170 s (excluding the first seven frames). We assume that a wave can be detected (and fitted) if 3/4 of a period is observed. Hence, sinusoidal motions with periods $\gtrsim$230 s cannot be detected here. Signatures of long-period waves could be detected through the non-periodic component of the fit, $g(t)$. The transverse displacement observed in this manner also appears to have relatively small velocity amplitudes. Furthermore, waves with periods between 200−500 s and amplitudes >3 km s^{-1} would displace the loops central axis by at least 100−400 km, something which would be measurable in both Hi-C and AIA, but is not seen.

Comparing an extended time-series taken from AIA with the short Hi-C time-series suggests that the period of time observed by Hi-C is representative of the dynamics in the structures studied, i.e., wave activity is low for extended periods of time. Small-amplitude wave activity is also observed in coronal structures identified only in AIA (1 and 2 in Fig. 1). Thus, our results suggest that transverse waves supported by some active region coronal structure may have small velocity amplitudes (<3 km s^{-1}) and would not provide a significant heating contribution.

Previous observational evidence for transverse waves in active regions was provided by measuring Doppler oscillations with Hinode EIS (Erdélyi & Taroyan 2008; Van Doorsselaere et al. 2010; Tian et al. 2012), reporting velocity amplitudes 1−2 km s^{-1} and periods of ∼300 s. If these previous observations are indeed signatures of transverse waves, they are consistent with our Hi-C and AIA amplitude measurements and our upper bound. These values are also consistent with CoMP results if we assume that a significant amount of wave energy (>90%) is unresolved in the CoMP data. As with previous studies, we are limited to the observation of a few active-region structures for a relatively short period of time. Our results hint that there may be categories of propagating transverse waves. Namely, waves with larger velocity amplitudes ($v > 3$ km s^{-1}) that are potentially excited by infrequent events that provide more energy flux (e.g., feature 3) than the driver of continuous (as suggested by CoMP results) small amplitude waves (<3 km s^{-1}). This idea is supported by our observations, with some structures demonstrating small-amplitude periodic motion (e.g., features A, B, 1, 2) and others displaying one to two periods of large-amplitude motion before the displacement becomes undetectable (feature 3). However, extended studies are required to confirm this.

Acknowledgements. R.M. is grateful to Northumbria University for the award of the Anniversary Fellowship and thanks A. Winebarger for useful discussions. The authors acknowledge IDL support provided by STFC. We acknowledge the High resolution Coronal imager instrument team for making the flight data publicly available. MSFC/NASA led the mission and partners include the Smithsonian Astrophysical Observatory in Cambridge, Mass; Lockheed Martin's Solar Astrophysical Laboratory in Palo Alto, Calif; the University of Central Lancashire in Lancashire, UK; and the Lebedev Physical Institute of the Russian Academy of Sciences in Moscow.

References

Aschwanden, M. J., & Schrijver, C. J. 2011, ApJ, 736, 102
Cirtain, J. W., Golub, L., Winebarger, A. R., et al. 2013, Nature, 493, 501
De Moortel, I., & Pascoe, D. J. 2012, ApJ, 746, 31
De Pontieu, B., McIntosh, S. W., Carlsson, M., et al. 2007, Science, 318, 1574
Erdélyi, R., & Taroyan, Y. 2008, A&A, 489, L49
Kuridze, D., Morton, R. J., Erdélyi, R., et al. 2012, ApJ, 750, 51
Lemen, J. R., Title, A. M., Akin, D. J., et al. 2011, Sol. Phys., 115
McIntosh, S. W., De Pontieu, B., Carlsson, M., et al. 2011, Nature, 475, 477
Morton, R. J., Verth, G., Jess, D. B., et al. 2012, Nat. Commun., 3, 1325
Pascoe, D. J., Hood, A. W., de Moortel, I., & Wright, A. N. 2012, A&A, 539, A37
Terradas, J., Goossens, M., & Verth, G. 2010, A&A, 524, A23
Tian, H., McIntosh, S. W., Wang, T., et al. 2012, ApJ, 759, 144
Tomczyk, S., & McIntosh, S. W., 2009, ApJ, 697, 1384
Tomczyk, S., McIntosh, S. W., Keil, S. L., et al. 2007, Science, 317, 1192
Van Doorsselaere, T., Nakariakov, V. M., Young, P. R., & Verwichte, E. 2008, A&A, 487, L17
Verth, G., Terradas, J., & Goossens, M. 2010, ApJ, 718, L102
Yuan, D., & Nakariakov, V. 2012, A&A, 543, A9

Appendix A: Online movies

The Hi-C sounding rocket took data on 12 July 2012 from 18:51:52 UT to 18:55:13 UT centred on an active region at (−130.″0, −453.″3) from disk centre. The images were obtained in the 193 Å passband (spectral width −5 Å). Data from the Solar Dynamic Observatory Atmospheric Imaging Assembly (SDO/AIA) were also used in our analysis. The AIA images are taken on the same day and show the time period 18:40:47−19:04:47 UT.

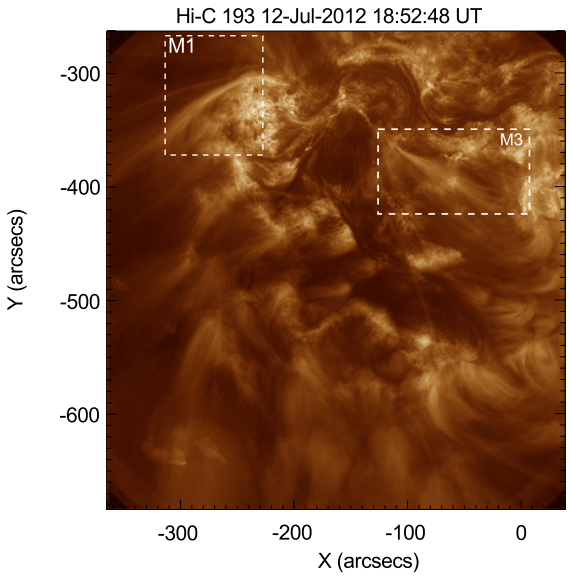

Fig. A.1. Active region as observed with Hi-C 193 Å. Movie 1 (M1) focuses on the coronal structure labelled A in the main text and parts Movie 3 (M3) focuses on the coronal structure labelled B in the manuscript. The boxes show the sub-regions of the Hi-C field of view in each movie.

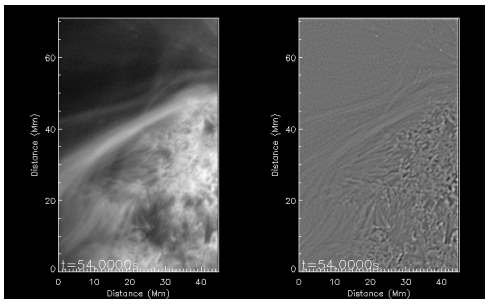

Fig. A.2. Still from Movie 1. The movie shows a unique view of coronal structures as seen with Hi-C (labelled A in the manuscript). The high resolution reveals fine-scale structure that is at the diffraction limit of SDO/AIA. Even though the time-series is short, it is possible to see flows and waves along these structures, in particular in the fibrils and the spicular features, some of which show enhanced emission. In contrast, the coronal structures do not show the same level of dynamic behaviour. Over the short time-scales (<200 s), little motion of the loops is observed, which is reflected by the measured small-amplitude transverse wave motion in the time-distance diagrams (Fig. 2 – main text). *The left panel* displays the log intensity images and *the right panel* shows the unsharp masked version.

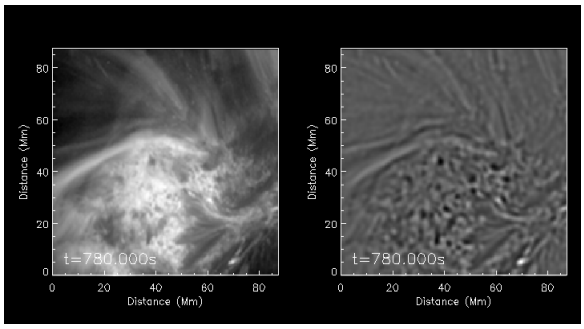

Fig. A.3. Still from Movie 2. The movie shows the same coronal structure as that in Movie 1 as observed with SDO/AIA in 193 Å. The field of view of the movie covers a slightly larger region than Movie 1. Comparing this to Movie 1, it can be seen that AIA does not resolve the fine structure seen in Hi-C. The time period that corresponds to the Hi-C data is between 660 s to 870 s.

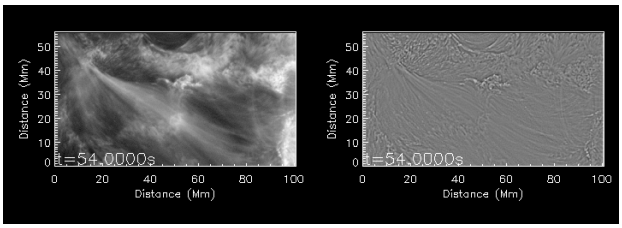

Fig. A.4. Still from Movie 3. The movie displays the coronal structure labelled B in the manuscript, observed with Hi-C. The absence of observable motion in the loop structure is reflected by the lack of measurable wave motion in the time-distance diagrams (Fig. 3 – main text).

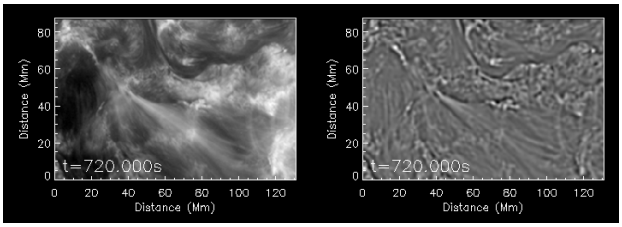

Fig. A.5. Still from Movie 4. The movie is of the same coronal structure as in Movie 3 but observed with AIA 193 Å. The field of view covers a slightly large region than that of Movie 3. The time period corresponding to the Hi-C data is from 660 s to 870 s.

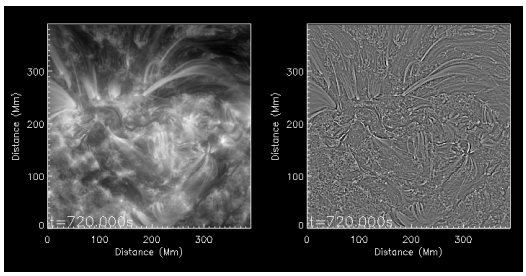

Fig. A.6. Still from Movie 5, showing the region observed by AIA 171 Å that is displayed in Fig. 1 in the main text. The coronal structures labelled A, B, 1, 2 and 3 are all visible in the movie. Note the visible motion in feature 3, in which the analysis finds relatively large velocity amplitude (>5 km s^{-1}) transverse displacements. This is compared with the other structures, where our analysis revealed only small velocity amplitudes.